中国机构CNS月报

02月刊

生物探索出品

目　录

一、导语

令国内科研界振奋的是，自然系列期刊在 2012 年的论文统计显示，发文 140 篇论文的中国科学院超过日本东京大学排名亚洲机构第一位，这也是 Nature Index 统计以来中国科研机构首次排名第一，反映出中国顶尖科研机构在数量上领跑亚洲。据生物探索统计，近 3 年内中国科研机构在 Nature、Cell 和 Science 三大系列期刊的总发文量逐渐上升， 由 2010 年的 140 篇上升到 2011 年的 199 篇，再升至 2012 年的 262 篇。在 2012 年，中国机构发文 Nature 系列期刊 157 篇，Cell 系列期刊 126 篇和 Science 系列期刊 73 篇。

在生物学领域，三大期刊（Cell、Nature 和 Science）及其子刊，简称 CNS，倍受中国研究人员推崇，他们希望凭借 CNS 在学术界的威望将中国最尖端、最前沿的研究成果向全世界传达。这些研究动态可谓是中国科研机构的最高水平。作者希望对此进行统计，以便于从发文成果追踪国内科研经费动向，同时，生物医药圈内的研究人员和学生可实时了解中国顶尖研究人员从事研究的的领域和方向。

二、2 月份中国机构发文 CNS 三大期刊

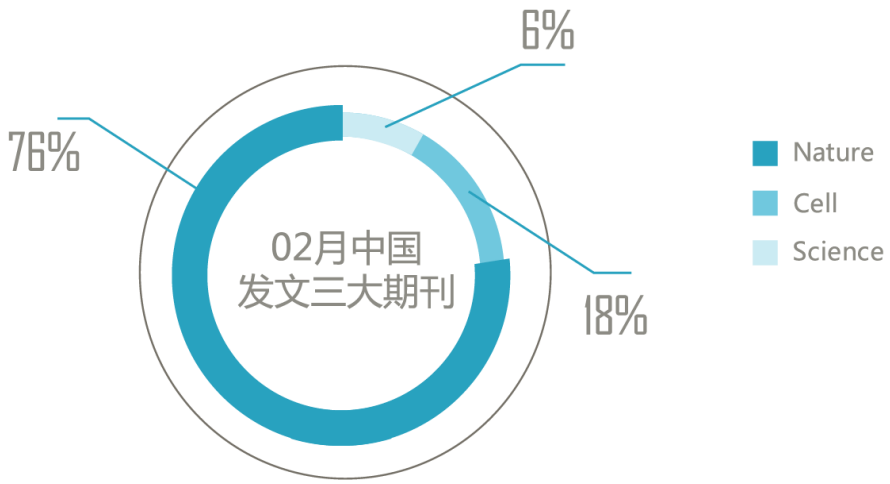

（饼状图表示期刊论文百分数）

2013年2月份中国研究机构在三大期刊及其子刊共发表33篇论文，包括Nature系列 25篇、Cell 系列6篇和Science系列2篇。其中Nature主刊的发文量是5篇，在Nature系列期刊上的比例是20%。从饼状图上可以看出，Nature系列刊贡献了中国研究机构CNS发文量的3/4以上，反映出中国研究机构青睐于Nature系列刊，这解释了Nature为迎合中国研究机构而在上海设立分支机构。

继1月份港台地区共发表5篇CNS论文之后，2013年2月份仅有台湾地区发表2篇CNS论文。在论文影响因子方面，台湾地区贡献了21.6分，约占总影响分子511分的4.2%。其余的31篇都源自中国大陆，这反映出其研究机构在CNS论文方面处于主体地位。

三、2月份学术领域热度

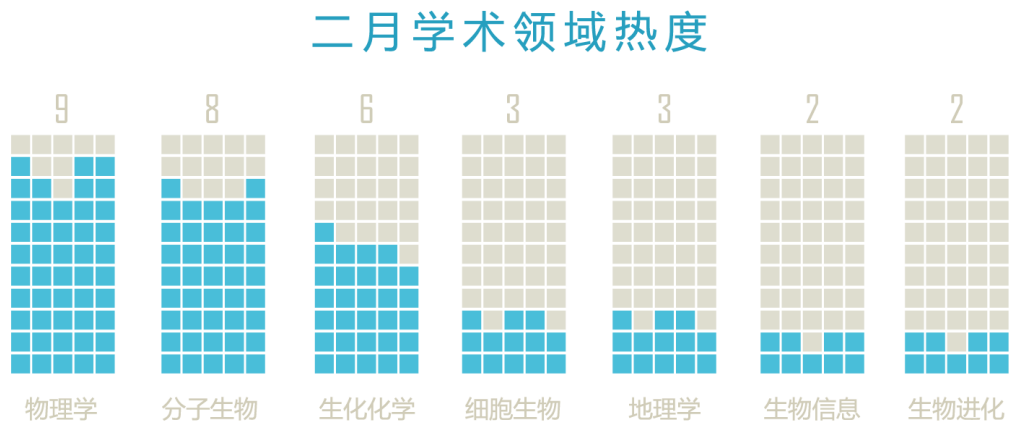

（柱状图反映论文数量/篇）

在2月份CNS刊登的中国研究论文中，物理学以10篇列于榜首，分子生物和生物化学分别位于第二、第三位。从来源上看，物理学论文全部来自Nature系列刊，可见Nature系列刊涉及的学术范围要比Cell、Science期刊的覆盖面广。

以基因组为对象的生物信息学研究持续成为热点，近6个月内中国研究机构都有关于基因组测序的CNS论文发表。2月份2篇生物信息学论文分别讲到中国树鼩和毛竹这2个物种的基因组。

四、2 月份城市&地区在 CNS 的论文和影响因子

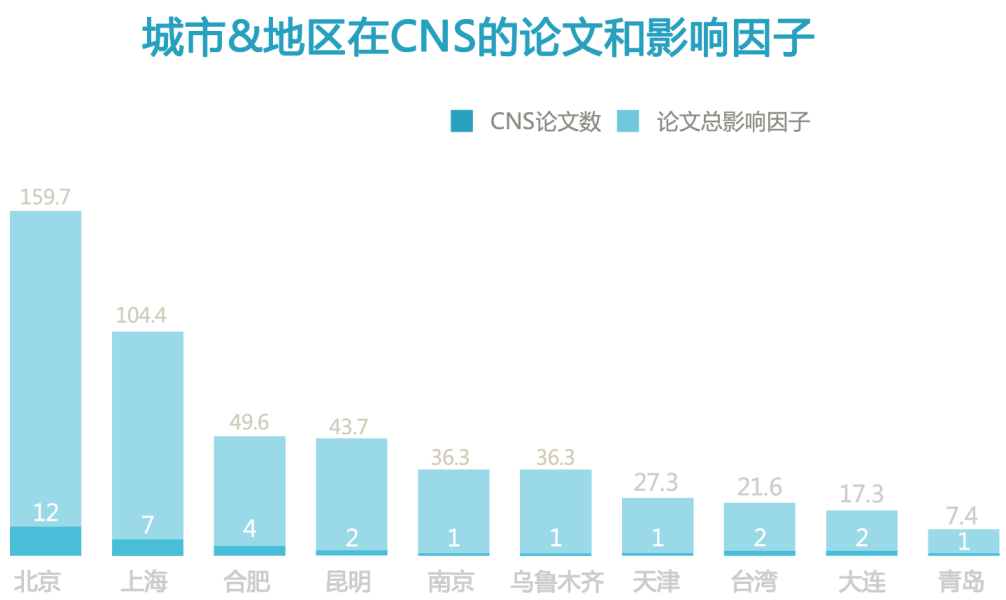

（影响因子源自 MedSci 查询系统，取小数点后一位）

从城市&地区来看，2 月份 CNS 论文影响因子超过 100 分的有北京和上海两地，北京以 159.7 分卫冕排行榜，较上月涨幅达 20.3 %。上月排名第 4 的上海跃居本月的第二位，其论文数由之前的 2 篇上升到 7 篇。从上图可以看出，北京的 CNS 论文影响因子遥遥领先其它城市&地区。

在 2 月份，合肥和昆明所获得的影响因子都处于 40-50 之间，而在平均影响因子这一参数上，发文仅 2 篇的昆明显然高于合肥；南京和乌鲁木齐两地都只发表 1 篇论文，不过由于发表在 Nature 主刊上，它们获得的影响因子分别高于发文 2 篇的台湾和大连两地的；另外，天津和青岛都发表一篇 CNS 论文。

对城市&地区的 CNS 影响因子统计，生物探索网站希望向用户提供关于地区研究水平的一项指数，让科研人员在从事各自研究领域的同时选择较高的研究平台和学术氛围。此外，由于论文来自不同的经费项目，因此城市&地区的 CNS 影响因子能从一个方面反映国家经费的分配比例。

五、2 月份中国机构发文 CNS 的走势

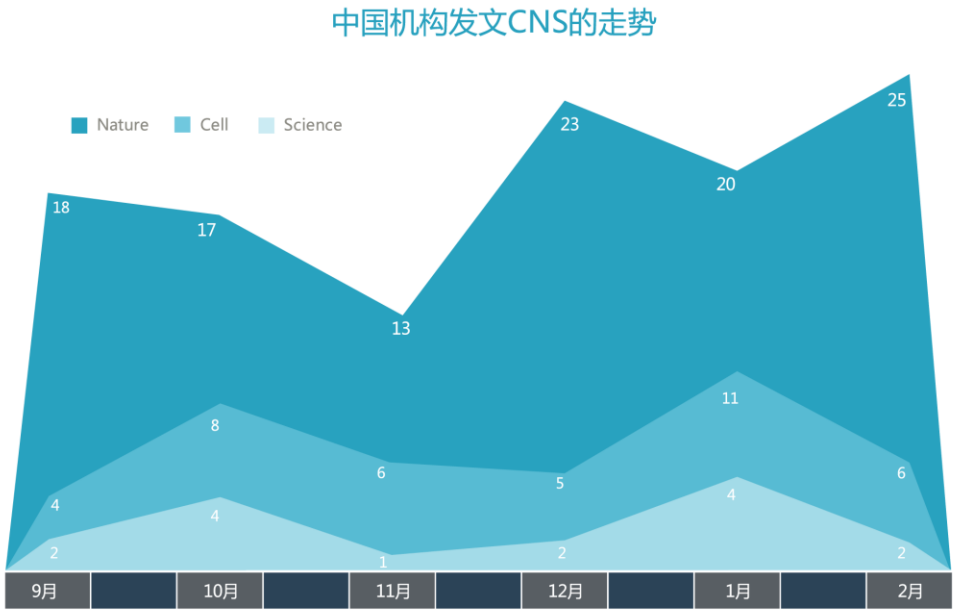

（数据统计源自 NCBI 网站 Pubmed）

在 2012 年 9 月至 2013 年 2 月之间中国机构发文 CNS 的统计结果中，数据表明：Nature 及其子刊发表的中国研究论文数量处于高位，总计 116 篇，其中 2 月最高达到 25 篇；相反，Science 及其子刊发表的中国研究论文数量处于低位，总计 15 篇，其中 11 月最低下落至 1 篇。

Nature 系列期刊的数量最多，它覆盖的学术类别和影响因子也较多，这是中国研究论文发表在 Nature 系列刊最多的原因之一；另一原因可能是，Nature 系列期刊对中国机构的研究成果认可度高，从 Nature 在上海设立编辑部一事可以看出，它对中国机构研究成果的重视。

六、2 月份 CNS 发文机构论文量统计

研究机构	CNS 论文		
	2 月份发文量	近 5 年总数	总数
中国科学院上海生命科学研究院	1	63	91
清华大学	1	57	72
北京大学	2	38	47
上海交通大学	2	29	33
中国科学技术大学	2	23	30
中国科学院遗传与发育生物学研究所	1	14	17
中国农业大学	1	11	17
中国科学院物理研究所	2	10	15
中国科学院大连化学物理研究所	1	10	14
中国科学院南京地质古生物研究所	1	4	12
安徽医科大学	2	8	8
山东大学	1	6	6
中国科学院大学	4	6	6
南开大学	1	6	6
中国科学院昆明动物研究所	1	4	5
云南大学	1	3	5
同济大学	1	3	4
华东理工大学	1	3	3
北京科技大学	1	2	2
中国科学院新疆生态与地理研究所	1	2	2
中国林业科学研究院	1	1	2
青岛大学	1	1	2
国立高雄师范大学	1	1	1

（数据源于 NCBI 网站 Pubmed）

从 2 月份 CNS 中国机构论文总数榜单上看，排名前三的分别中国科学院上海生命科学研究院、清华大学和北京大学。发表 1 篇 CNS 论文以上的研究机构是北京大学、上海交通大学、中国科学技术大学、中国科学院物理研究所、安徽医科大学和中国科学院大学，其中中国科学院大学发表了 4 篇，是本月最高发文量的学术机构。

在 2 月份 CNS 论文的统计数据中，除中国科学院南京地质古生物研究所之外，中国机构近 5 年发表的 CNS 论文总数全都不低于其 CNS 论文总数的一半，这表明近 5 年来中国机构发文 CNS 的速度和数量增加较快；2 月份，仅有国立高雄师范大学首次发文 CNS，除首次发

文 CNS 的研究机构外，安徽医科大学、山东大学、中国科学院大学、南开大学、华东理工大学、北京科技大学和中国科学院新疆生态与地理研究所发表的CNS论文全都在近5年内。

七、2 月份 CNS 论文通讯作者的项目数和经费

研究机构	通讯作者	项目金额/万	项目数/个
中国科学院大连化学物理研究所	李灿	3452.4	29
中国农业大学	张福锁	2130.7	23
中国科学技术大学	田志刚	1909	15
中国科学院大连化学物理研究所	邹汉法	1515.9	19
北京大学	刘忠范	1295.6	14
中国林业科学研究院	韩斌	1220	3
上海交通大学	张大兵	1003.9	7
中国科学院物理研究所	靳常青	863.1	12
中国科学院遗传与发育生物学研究所	左建儒	805.8	7
清华大学	李景虹	488	6
深圳华大基因研究院	王俊	470	3
青岛大学	谢俊霞	381	12
中国科学院昆明动物研究所	姚永刚	360	3
华东理工大学	龙亿涛	300.6	4
中国科学技术大学	魏海明	237	6
同济大学	周怀阳	223	4
云南大学	张喜光	217.9	5
上海交通大学	臧敬五	212.6	4
中国科学院南京地质古生物研究所	黄迪颖	210.2	9
北京大学	彭海琳	197	3
北京大学	王克威	197	2
中国科学院物理研究所	胡勇胜	136	2
青岛大学	姜宏	122	3
中国林业科学研究院	江泽慧	100	1
山东大学威海分校	史全岐	72	2
安徽医科大学	张旭东	58	2

（数据源于 NSFC）

对于 2 月份中国机构发文 CNS 的 26 位通讯作者（统计量不完全），国家自然科学基金项目提供了详细的项目金额和数量。中国科学院大连化学物理研究所的李灿教授以 3452.4 万元高举榜首，项目数为 29 个；中国农业大学的张福锁教授和中国科学技术大学的田志刚教授以 2130.7 万和 1909 万分列第二、三名，他们的项目数分别为 23 和 15 个。

排名前 10 的通讯作者分别来自北京（6 位）、大连（2 位）、上海（1 位）和合肥（1 位），其中，北京地区 6 位通讯作者位于项目金额榜前十位之内，这反映出北京位列 2 月份 CNS 中国机构影响因子之首的经费基础。

八、广受评议的研究

Biomimetic enzyme nanocomplexes and their use as antidotes and preventive measures for alcohol intoxication.（TheScientist 网站报道标题为 Buffering Against Alcohol）

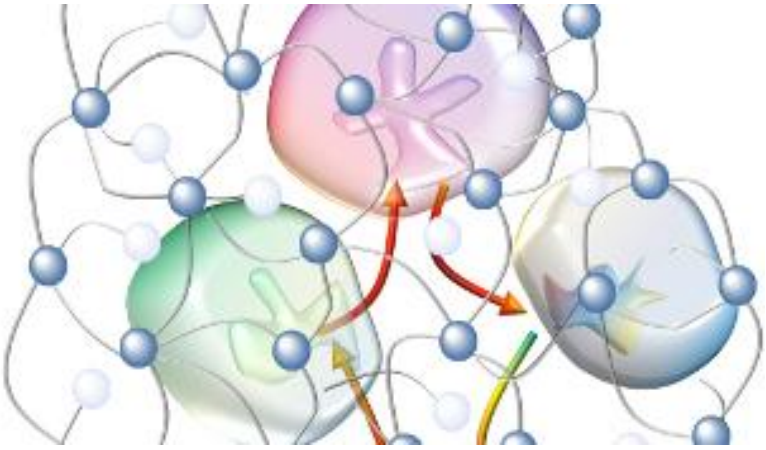

南开大学、加州大学洛杉矶分校等处的研究人员，采用了一种新技术组合多种功能酶，从而能用于减少血液中的酒精浓度，以及肝脏损伤。

荷兰 Radboud 大学的有机生化教授 Jan van Hest 没有参与该研究，他说：“这一精妙方法在可控制条件下定位酶的位置，在该领域算得上迈出重要的一步。由于在活体系统中表现出较高的活性，多酶复合体已提供了很好地实验结果，有望成为一种可应用于其它用途的通用方法。”

他补充道：“在酶的定位组装中，较为困难的是分子水平上的操作控制，不过如果你希望催化级联反应，这一困难是无法回避的，毕竟它发挥重要作用。研究人员所进行的精妙操作就是，通过操纵 DNA 支架位置以封装多个聚合体，这一技术能更多地控制酶的组合，从而改变之前酶的无序组合。”

加州大学洛杉矶分校的卢云峰教授称：“这一药丸（多酶复合体）所执行的功能非常类似于肝脏功能，通过进一步研究，这一发现有望用于预防酒精中毒，甚至能作为预防酒精中毒的解酒药。”

南开大学化学学院高分子化学研究所史林启教授表示，这种将不同酶复合在一起的技术很有意义，他们还将继续开发，并拟在癌症治疗等重大问题中应用这项技术。

九、专家精选

Structure of the MST4 in Complex with MO25 Provides Insights into Its Activation Mechanism.（中国科学院上海生命科学研究院）

中国科学院上海生物化学与细胞生物学研究所周兆才（左图）和赵允研究组的最新研究，从生物化学和细胞生物学等多个角度阐述了支架蛋白 MO25 对 STE20 家族激酶 MST4 的激活机制。相关成果公布在 Cell 杂志《Structure》期刊上。

在本项研究中，周兆才实验室的史竹兵，焦石和张振等人对 MST4-MO25 复合物进行了晶体结构分析，并在结构指导下通过突变学研究从生物化学与细胞生物学等多个角度对 MO25 激活 MST4 的机制以及 MST4-MO25 复合物的生物学功能进行了阐释。通过对 MST4-MO25 晶体结构的分析，并对其与 MST4 以及相关激酶单独结构的比较，我们发现 MO25 的结合引起 MST4 的关键元件αC 螺旋的构象发生显著变化，使得 MST4 处于激活状态。通过对晶体结构中 MST4 二聚化的分析，揭示了 MST4 自身磷酸化的机制。体外的动力学实验，激酶活性实验以及体内细胞凋亡实验表明，MO25 在细胞内与 MST4 结合并激活 MST4 从而促进细胞凋亡的发生。

在周兆才和赵允研究员的指导下的这项研究，为进一步探索 MO25 对 STE20 家族其他激酶的激活提供了结构生物学基础。该研究工作得到科技部、国家自然科学基金委、上海市科委以及中科院的经费资助。

Genome of the Chinese tree shrew.（中国科学院昆明动物研究所）

中科院昆明动物所姚永刚教授（左图）和华大基因研究院等单位合作完成了树鼩基因组的破译工作，通过完成高质量的树鼩（Tupaia belangeri chinensis）全基因组测序及比较基因组分析，阐明了其系统分类地位和相关生物学特征的遗传基础。相关成果发表在《自然通讯》（Nature Communication）杂志上。

研究人员利用二代测序技术完成一只来自云南的树鼩的全基因组测序，总覆盖度高达 79X。之后与多个物种基因组进行了比较分析，从全基因组基因序列比较角度重构了树鼩与其他物种的系统发育关系，证实了树鼩与灵长类亲缘关系最为接近。这一研究结果从基因组水平上解决了树鼩分类学方面的争论，为其在很多方面代替非人灵长类动物作为实验动物模型提供了重要依据。经过进一步分析树鼩与灵长类之间的遗传学关系，研究人员共鉴定出 28 个树鼩与灵长类共有的功能性基因。之前的研究认为这些基因属灵长类特有。

研究人员还对树鼩基因组中的药物作用靶点基因进行了研究，例如细胞色素 P450 超家族能够编码一些与药物代谢、活化和相互作用相关的一些酶。树鼩拥有与人类非常接近的细胞色素 P450 超家族的组成结构和基因一致性。研究人员对人类和树鼩的肝炎药物靶点基因进行研究后发现二者同源度很高。这种药物靶点以及相关信号通路的保守性，使得树鼩更好的用于评价用于药物分布、药物靶点、药代动力学以及药物副作用研究。

Phosphorylation of FOXP3 controls regulatory T cell function and is inhibited by TNF-α in rheumatoid arthritis.（上海交通大学）

上海交通大学医学院的臧敬五教授（左图）最新研究，揭示了类风湿关节炎的新疾病分子机理。证实在类风湿关节炎中 TNF-α 抑制 FOXP3 磷酸化，导致了调节性 T 细胞功能受损。研究成果发表在 2 月 10 日的《自然医学》（Nature medicine）杂志上。

在这篇论文中，研究人员证实 forkhead box P3 (FOXP3)转录活性，及 Treg 细胞抑制功能均受到 FOXP3 C-末端 DNA 结合域 Ser418 位点磷酸化作用的调控。研究人员发现在类风湿性关节炎炎症滑膜中，肿瘤坏死因子α (TNF-α)会诱导蛋白磷酸酶 1 表达及酶活性。在来自患者的 Treg 细胞中，他们证实 PP1 使得 FOXP3 的 Ser418 位点特异性去磷酸化，从而导致了 Treg 细胞功能受损。

研究结果表明在类风湿关节炎患者的滑膜中 TNF-α 通过 FOXP3 去磷酸化作用维持了 Treg 细胞和致病 TH17 及 TH1 细胞之间的平衡。由此，为我们指出了与 TNFα 有关的疾病的一种新的治疗标靶，为治疗此类疾病提供了一种新思路。

MicroRNA-92a Upholds Bmp Signaling by Targeting noggin3 during Pharyngeal Cartilage Formation.（中国科学院动物研究所）

中国科学院动物研究所王强研究员（左图）和孟安明院士在发育生物学著名杂志《Developmental Cell》合作发表了 mir-92a 调控斑马鱼咽部软骨形成的重要研究进展。这有助于理解一类常见的胎儿出生缺陷——颅面畸形——的遗传机制。

研究发现，MicroRNA 通过多种方式调节靶基因的表达而在个体发育和生理病理过程中发挥重要作用。miR-92a 在斑马鱼咽部表达，主要通过维持咽部骨形成蛋白 Bmp 的信号强度而保障咽部软骨的正常发育。miR-92a 可与咽部表达的 Bmp 拮抗因子 Noggin3 的 mRNA 结合，导致其降解，从而解除对 Bmp 信号的抑制作用。当用吗啉环修饰的反义寡核苷酸抑制斑马鱼胚胎中 miR-92a 的活性时，noggin3 的 mRNA 稳定性增高，致使 Bmp 信号不足，导致软骨前体细胞不能正常增殖、分化，造成严重的咽部软骨缺失；相反，

在胚胎中注射合成的 miR-92a，可促进 noggin3 的 mRNA 的降解，使得 Bmp 信号在咽部软骨区域活性过高，触发细胞凋亡。

该项研究从发育生物学的角度阐明，在咽部软骨发育过程中，Bmp 信号的活性必须受到精密调控，活性过高或过低都会导致软骨发育缺陷。而 mir-92a 就是我们鉴定到的调控 Bmp 信号活性的关键因子。miR-92a 在软骨发育中的研究进展，增进了我们对软骨发育机制的认识，加深了对相关软骨疾病发病机理的理解，为建立新的防治策略和诊疗方法奠定理论基础。

Structural Insight into Inactivation of Plasminogen Activator Inhibitor-1 by a Small-Molecule Antagonist (中国科学院福建物质结构研究所)

中国科学院福建物质结构研究所黄明东研究员课题组在针对抗血栓、抗肿瘤重要靶标——纤溶酶原激活物抑制因子 1（PAI-1）的药物设计研究取得进展。研究通过药物筛选发现了一个 PAI-1 的小分子抑制剂，并以 X-射线晶体学手段揭示了其在 PAI-1 蛋白分子上的药物结合口袋，阐述了药物作用机理，为以 PAI-1 为靶标的药物发现和药物设计提供了新的思路和结构基础。

黄明东研究员课题组通过与中国科学院上海药物研究所胡立宏研究员课题组合作，从天然产物库中筛选获得了一个选择性的 PAI-1 小分子抑制剂——信筒子醌（embelin，IC50～1.6 μM）。研究还通过 X-射线晶体学方法，解析了 PAI-1 蛋白与该小分子的复合物晶体结构，揭示了信筒子醌在 PAI-1 分子上的药物结合口袋。进一步研究表明，信筒子醌对 PAI-1 的抑制作用是通过两种作用方式实现：首先，信筒子醌作用于 PAI-1 蛋白上 β -strand 2A, a-helix D、E 及 F 上的氨基酸残基，阻碍了 PAI-1 的反应中心环（RCL）的插入，从而快速地诱导 PAI-1 转换成底物态的无活性形式；其次，信筒子醌还会使 PAI-1 聚集而导致活性丧失。该项研究从原子水平上揭示 PAI-1 分子的药物结合口袋及药物抑制机理，为进一步的药物发现和理性药物设计提供了重要的线索和依据。

信筒子醌来源于紫金牛，始载于宋。《图经本草》记载："紫金牛，生福州，味辛，叶如茶，上绿下紫，实圆，红如丹朱，根微紫色，八月采，去心暴干，颇似巴戟"。《本草纲目》载紫

金牛有"解毒破血"功能。紫金牛又名矮地茶，民间用于肺痿、咳嗽及火眼等。本项研究证实了信筒子醌有一定的溶栓效果。

十、2 月份论文列表

1、Nature 及其子刊

On-demand semiconductor single-photon source with near-unity indistinguishability. [地址链接**]**

通讯作者：Pan JW. (中国科学技术大学) Nat Nanotechnol. 2013 Mar;8(3):213-7.

Single-photon sources based on semiconductor quantum dots offer distinct advantages for quantum information, including a scalable solid-state platform, ultrabrightness and interconnectivity with matter qubits. A key prerequisite for their use in optical quantum computing and solid-state networks is a high level of efficiency and indistinguishability. Pulsed resonance fluorescence has been anticipated as the optimum condition for the deterministic generation of high-quality photons with vanishing effects of dephasing. Here, we generate pulsed single photons on demand from a single, microcavity-embedded quantum dot under s-shell excitation with 3 ps laser pulses. The π pulse-excited resonance-fluorescence photons have less than 0.3% background contribution and a vanishing two-photon emission probability. Non-postselective Hong-Ou-Mandel interference between two successively emitted photons is observed with a visibility of 0.97(2), comparable to trapped atoms and ions. Two single photons are further used to implement a high-fidelity quantum controlled-NOT gate.

Genome of the Chinese tree shrew. [地址链接**]**

通讯作者：姚永刚 (中国科学院昆明动物研究所&中国科学院大学) Nat Commun. 2013;4:1426.

Chinese tree shrews (Tupaia belangeri chinensis) possess many features valuable in animals used as experimental models in biomedical research. Currently, there are numerous attempts to employ tree shrews as models for a variety of human disorders: depression, myopia, hepatitis B and C virus infections, and hepatocellular carcinoma, to name a few. Here we present a publicly available annotated genome sequence for the Chinese tree shrew. Phylogenomic analysis of the tree shrew and other mammalians highly support its close affinity to primates. By characterizing key factors and signalling pathways in nervous and immune systems, we demonstrate that tree shrews possess both shared common and unique features, and provide a genetic basis for the use of this animal as a potential model for biomedical research.

Spatial separation of photogenerated electrons and holes among {010} and {110} crystal

facets of BiVO(4). [地址链接**]**

通讯作者：李灿 (中国科学院大连化学物理研究所%中国科学院大学) Nat Commun. 2013;4:1432.

Charge separation is crucial for increasing the activity of semiconductor-based photocatalysts, especially in water splitting reactions. Here we show, using monoclinic bismuth vanadate crystal as a model photocatalyst, that efficient charge separation can be achieved on different crystal facets, as evidenced by the reduction reaction with photogenerated electrons and oxidation reaction with photogenerated holes, which take place separately on the {010} and {110} facets under photo-irradiation. Based on this finding, the reduction and oxidation cocatalysts are selectively deposited on the {010} and {110} facets respectively, resulting in much higher activity in both photocatalytic and photoelectrocatalytic water oxidation reactions, compared with the photocatalyst with randomly distributed cocatalysts. These results show that the photogenrated electrons and holes can be separated between the different facets of semiconductor crystals. This finding may be useful in semiconductor physics and chemistry to construct highly efficient solar energy conversion systems.

Peptide hormone ghrelin enhances neuronal excitability by inhibition of Kv7/KCNQ channels. [地址链接**]**

通讯作者：王克威&姜宏&谢俊霞 (青岛大学) Nat Commun. 2013;4:1435.

The gut-derived orexigenic peptide hormone ghrelin enhances neuronal firing in the substantia nigra pars compacta, where dopaminergic neurons modulate the function of the nigrostriatal system for motor coordination. Here we describe a novel mechanism by which ghrelin enhances firing of nigral dopaminergic neurons by inhibiting voltage-gated potassium Kv7/KCNQ/M-channels through its receptor GHS-R1a and activation of the PLC-PKC pathway. Brain slice recordings of substantia nigra pars compacta neurons reveal that ghrelin inhibits native Kv7/KCNQ/M-currents. This effect is abolished by selective inhibitors of GHS-R1a, PLC and PKC. Transgenic suppression of native Kv7/KCNQ/M-channels in mice or channel blockade with XE991 abolishes ghrelin-induced hyperexcitability. In vivo, intracerebroventricular ghrelin administration causes increased dopamine release and turnover in the striatum. Microinjection of ghrelin or XE991 into substantia nigra pars compacta results in contralateral dystonic posturing, and attenuation of catalepsy elicited by systemic administration of the D2 receptor antagonist haloperidol. Our findings indicate that the ghrelin/KCNQ signalling is likely a common pathway utilized by the nervous system.

New diluted ferromagnetic semiconductor with Curie temperature up to 180 K and isostructural to the '122' iron-based superconductors. [地址链接**]**

通讯作者：靳常青 (中国科学院物理研究所) Nat Commun. 2013;4:1442.

Diluted magnetic semiconductors have received much attention due to their potential applications

for spintronics devices. A prototypical system (Ga,Mn)As has been widely studied since the 1990s. The simultaneous spin and charge doping via hetero-valent (Ga(3+),Mn(2+)) substitution, however, resulted in severely limited solubility without availability of bulk specimens. Here we report the synthesis of a new diluted magnetic semiconductor (Ba(1-x)K(x))(Zn(1-y)Mn(y))(2)As(2), which is isostructural to the 122 iron-based superconductors with the tetragonal ThCr(2)Si(2) (122) structure. Holes are doped via (Ba(2+), K(1+)) replacements, while spins via isovalent (Zn(2+),Mn(2+)) substitutions. Bulk samples with x=0.1-0.3 and y=0.05-0.15 exhibit ferromagnetic order with T(C) up to 180 K, which is comparable to the highest T(C) for (Ga,Mn)As and significantly enhanced from T(C) up to 50 K of the '111'-based Li(Zn,Mn)As. Moreover, ferromagnetic (Ba,K)(Zn,Mn)(2)As(2) shares the same 122 crystal structure with semiconducting BaZn(2)As(2), antiferromagnetic BaMn(2)As(2) and superconducting (Ba,K)Fe(2)As(2), which makes them promising for the development of multilayer functional devices.

Janus graphene from asymmetric two-dimensional chemistry. [地址链接**]**

通讯作者：彭海琳&刘忠范(北京大学) Nat Commun. 2013;4:1443.

Janus materials have distinct surfaces on their opposite faces. Graphene, a two-dimensional giant molecule, provides an excellent candidate to fabricate the thinnest Janus discs and study the asymmetric chemistry of atomic-thick nanomembranes using covalent chemical functionalisation. Here we present the first experimental realisation of nonsymmetrically modified single-layer graphene--Janus graphene--which is fabricated by a two-step surface covalent functionalisation assisted by a poly(methyl methacrylate)-mediated transfer approach. Four types of Janus graphene are produced by co-grafting of halogen and aryl/oxygen-functional groups on each side. Chemical decorations on one side are found to be capable of affecting both chemical reactivity and physical wettability of the opposite side, indicative of communication between the two grafted groups. This novel asymmetric structure provides a platform for theoretical and experimental studies of two-dimensional chemistry and graphene devices with multiple functions.

EAT1 promotes tapetal cell death by regulating aspartic proteases during male reproductive development in rice. [地址链接**]**

通讯作者：张大兵 (上海交通大学) Nat Commun. 2013;4:1445.

Programmed cell death is essential for the development of multicellular organisms, yet pathways of plant programmed cell death and its regulation remain elusive. Here we report that ETERNAL TAPETUM 1, a basic helix-loop-helix transcription factor conserved in land plants, positively regulates programmed cell death in tapetal cells in rice anthers. eat1 exhibits delayed tapetal cell death and aborted pollen formation. ETERNAL TAPETUM 1 directly regulates the expression of OsAP25 and OsAP37, which encode aspartic proteases that induce programmed cell death in both yeast and plants. Expression and genetic analyses revealed that ETERNAL TAPETUM 1 acts downstream of TAPETUM DEGENERATION RETARDATION, another positive regulator of tapetal programmed cell death, and that ETERNAL TAPETUM 1 can also interact with the

TAPETUM DEGENERATION RETARDATION protein. This study demonstrates that ETERNAL TAPETUM 1 promotes aspartic proteases triggering plant programmed cell death, and reveals a dynamic regulatory cascade in male reproductive development in rice.

Thin crust as evidence for depleted mantle supporting the Marion Rise. [地址链接]

通讯作者：周怀阳 (同济大学) Nature. 2013 Feb 14;494(7436):195-200.

The global ridge system is dominated by oceanic rises reflecting large variations in axial depth associated with mantle hotspots. The little-studied Marion Rise is as large as the Icelandic Rise, considering both length and depth, but has an axial rift (rather than a high) nearly its entire length. Uniquely along the Southwest Indian Ridge systematic sampling allows direct examination of crustal architecture over its full length. Here we show that, unlike the Icelandic Rise, peridotites are extensively exposed high on the rise, revealing that the crust is generally thin, and often missing, over a rifted rise. Therefore the Marion Rise must be largely an isostatic response to ancient melting events that created low-density depleted mantle beneath the Southwest Indian Ridge rather than thickened crust or a large thermal anomaly. The origin of this depleted mantle is probably the mantle emplaced into the African asthenosphere during the Karoo and Madagascar flood basalt events.

Investigating electron-transfer processes using a biomimetic hybrid bilayer membrane system. [地址链接]

通讯作者：龙亿涛 (华东理工大学) Nat Protoc. 2013 Mar;8(3):439-50

Here we report a protocol to investigate the electron-transfer processes of redox-active biomolecules in biological membranes by electrochemistry using biomimetic hybrid bilayer membranes (HBMs) assembled on gold electrodes. Redox-active head groups, such as the ubiquinone moiety, are embedded in HBMs that contain target molecules, e.g., nicotinamide adenine dinucleotide (NADH). By using this approach, the electron-transfer processes between redox molecules and target biomolecules are mediated by mimicking the redox cycling processes in a natural membrane. Also included is a procedure for in situ surface-enhanced Raman scattering (SERS) to confirm the electrochemically induced conformational changes of the target biomolecules in the HBMs. In addition, each step in constructing the HBMs is characterized by electrochemical impedance spectroscopy (EIS), high-resolution X-ray photoelectron spectroscopy (XPS) and atomic force microscopy (AFM). The time required for the entire protocol is ~12 h, whereas the electrochemical measurement of electron-transfer processes takes less than 1 h to complete.

Robust phosphoproteome enrichment using monodisperse microsphere-based immobilized titanium (IV) ion affinity chromatography. [地址链接]

通讯作者：邹汉法 (中国科学院大连化学物理研究所) Nat Protoc. 2013 Mar;8(3):461-80

Mass spectrometry (MS)-based proteomics has become the preferred tool for the analysis of protein phosphorylation. To be successful at such an endeavor, there is a requirement for an efficient enrichment of phosphopeptides. This is necessary because of the substoichiometric nature of phosphorylation at a given site and the complexity of the cell. Recently, new alternative materials have emerged that allow excellent and robust enrichment of phosphopeptides. These monodisperse microsphere-based immobilized metal ion affinity chromatography (IMAC) resins incorporate a flexible linker terminated with phosphonate groups that chelate either zirconium or titanium ions. The chelated zirconium or titanium ions bind specifically to phosphopeptides, with an affinity that is similar to that of other widely used metal oxide affinity chromatography materials (typically TiO(2)). Here we present a detailed protocol for the preparation of monodisperse microsphere-based Ti(4+)-IMAC adsorbents and the subsequent enrichment process. Furthermore, we discuss general pitfalls and crucial steps in the preparation of phosphoproteomics samples before enrichment and, just as importantly, in the subsequent mass spectrometric analysis. Key points such as lysis, preparation of the chromatographic system for analysis and the most appropriate methods for sequencing phosphopeptides are discussed. Bioinformatics analysis specifically relating to site localization is also addressed. Finally, we demonstrate how the protocols provided are appropriate for both single-protein analysis and the screening of entire phosphoproteomes. It takes ~2 weeks to complete the protocol: 1 week to prepare the Ti(4+)-IMAC material, 2 d for sample preparation, 3 d for MS analysis of the enriched sample and 2 d for data analysis.

Phosphorylation of FOXP3 controls regulatory T cell function and is inhibited by TNF-α in rheumatoid arthritis. [地址链接**]**

通讯作者：臧敬五(上海交通大学)Nat Med. 2013 Feb 10;19(3):322-8

Regulatory T (T) cells suppress autoimmune disease, and impaired T cell function is associated with rheumatoid arthritis. Here we demonstrate that forkhead box P3 (FOXP3) transcriptional activity and, consequently, T cell suppressive function are regulated by phosphorylation at Ser418 in the C-terminal DNA-binding domain. In rheumatoid arthritis-derived T cells, the Ser418 site was specifically dephosphorylated by protein phosphatase 1 (PP1), whose expression and enzymatic activity were induced in the inflamed synovium by tumor necrosis factor α (TNF-α), leading to impaired T cell function. Moreover, TNF-α-induced T cell dysfunction correlated with increased numbers of interleukin-17 (IL-17) and interferon-γ (IFN-γ)CD4 T cells within the inflamed synovium in rheumatoid arthritis. Treatment with a TNF-α-specific antibody restored T cell function in subjects with rheumatoid arthritis, which was associated with decreased PP1 expression and increased FOXP3 phosphorylation in T cells. Thus, TNF-α controls the balance between T cells and pathogenic T17 and T1 cells in the synovium of individuals with rheumatoid arthritis through FOXP3 dephosphorylation.

Solar wind entry into the high-latitude terrestrial magnetosphere during geomagnetically quiet times. [地址链接**]**

通讯作者：史全岐 (山东大学威海分校) Nat Commun. 2013 Feb 12;4:1466

An understanding of the transport of solar wind plasma into and throughout the terrestrial magnetosphere is crucial to space science and space weather. For non-active periods, there is little agreement on where and how plasma entry into the magnetosphere might occur. Moreover, behaviour in the high-latitude region behind the magnetospheric cusps, for example, the lobes, is poorly understood, partly because of lack of coverage by previous space missions. Here, using Cluster multi-spacecraft data, we report an unexpected discovery of regions of solar wind entry into the Earth's high-latitude magnetosphere tailward of the cusps. From statistical observational facts and simulation analysis we suggest that these regions are most likely produced by magnetic reconnection at the high-latitude magnetopause, although other processes, such as impulsive penetration, may not be ruled out entirely. We find that the degree of entry can be significant for solar wind transport into the magnetosphere during such quiet times.

IGF-1 promotes the development and cytotoxic activity of human NK cells. [地址链接**]**

通讯作者：魏海明&田志刚 (中国科技大学&安徽医科大学) Nat Commun. 2013 Feb 12;4:1479.

Insulin-like growth factor 1 (IGF-1) is a critical regulator of many physiological functions, ranging from longevity to immunity. However, little is known about the role of IGF-1 in natural killer cell development and function. Here, we identify an essential role for IGF-1 in the positive regulation of human natural killer cell development and cytotoxicity. Specifically, we show that human natural killer cells have the ability to produce IGF-1 and that differential endogenous IGF-1 expression leads to disparate cytotoxicity in human primary natural killer cells. Moreover, miR-483-3p is identified as a critical regulator of IGF-1 expression in natural killer cells. Overexpression of miR-483-3p has an effect similar to IGF-1 blockade and decreased natural killer cell cytotoxicity, whereas inhibition of miR-483-3p has the opposite effect, which is reversible with IGF-1 neutralizing antibody. These findings indicate that IGF-1 and miR-483-3p belong to a new class of natural killer cell functional modulators and strengthen the prominent role of IGF-1 in innate immunity.

A new class of Solvent-in-Salt electrolyte for high-energy rechargeable metallic lithium batteries. [地址链接**]**

通讯作者：胡勇胜 (中国科学院物理研究所) Nat Commun. 2013 Feb 12;4:1481.

Liquid electrolyte plays a key role in commercial lithium-ion batteries to allow conduction of lithium-ion between cathode and anode. Traditionally, taking into account the ionic conductivity, viscosity and dissolubility of lithium salt, the salt concentration in liquid electrolytes is typically less than 1.2 mol l(-1). Here we show a new class of 'Solvent-in-Salt' electrolyte with ultrahigh salt concentration and high lithium-ion transference number (0.73), in which salt holds a dominant position in the lithium-ion transport system. It remarkably enhances cyclic and safety performance of next-generation high-energy rechargeable lithium batteries via an effective suppression of lithium dendrite growth and shape change in the metallic lithium anode. Moreover, when used in

lithium-sulphur battery, the advantage of this electrolyte is further demonstrated that lithium polysulphide dissolution is inhibited, thus overcoming one of today's most challenging technological hurdles, the 'polysulphide shuttle phenomenon'. Consequently, a coulombic efficiency nearing 100% and long cycling stability are achieved.

Biomimetic enzyme nanocomplexes and their use as antidotes and preventive measures for alcohol intoxication. [地址链接]

通讯作者：Lu Y. (南开大学) Nat Nanotechnol. 2013 Mar;8(3):187-92.

Organisms have sophisticated subcellular compartments containing enzymes that function in tandem. These confined compartments ensure effective chemical transformation and transport of molecules, and the elimination of toxic metabolic wastes. Creating functional enzyme complexes that are confined in a similar way remains challenging. Here we show that two or more enzymes with complementary functions can be assembled and encapsulated within a thin polymer shell to form enzyme nanocomplexes. These nanocomplexes exhibit improved catalytic efficiency and enhanced stability when compared with free enzymes. Furthermore, the co-localized enzymes display complementary functions, whereby toxic intermediates generated by one enzyme can be promptly eliminated by another enzyme. We show that nanocomplexes containing alcohol oxidase and catalase could reduce blood alcohol levels in intoxicated mice, offering an alternative antidote and prophylactic for alcohol intoxication.

Amphibious flies and paedomorphism in the Jurassic period. [地址链接]

通讯作者：黄迪颖(中国科学院南京地质古生物研究所) Nature. 2013 Mar 7;495(7439):94-7

The species of the Strashilidae (strashilids) have been the most perplexing of fossil insects from the Jurassic period of Russia and China. They have been widely considered to be ectoparasites of pterosaurs or feathered dinosaurs, based on the putative presence of piercing and sucking mouthparts and hind tibio-basitarsal pincers purportedly used to fix onto the host's hairs or feathers. Both the supposed host and parasite occur in the Daohugou beds from the Middle Jurassic epoch of China (approximately 165 million years ago). Here we analyse the morphology of strashilids from the Daohugou beds, and reach markedly different conclusions; namely that strashilids are highly specialized flies (Diptera) bearing large membranous wings, with substantial sexual dimorphism of the hind legs and abdominal extensions. The idea that they belong to an extinct order is unsupported, and the lineage can be placed within the true flies. In terms of major morphological and inferred behavioural features, strashilids resemble the recent (extant) and relict members of the aquatic fly family Nymphomyiidae. Their ontogeny are distinguished by the persistence in adult males of larval abdominal respiratory gills, representing a unique case of paedomorphism among endopterygote insects. Adult strashilids were probably aquatic or amphibious, shedding their wings after emergence and mating in the water.

Enhanced nitrogen deposition over China. [地址链接]

通讯作者：张福锁(中国农业大学) Nature. 2013 Feb 28;494(7438):459-62.

China is experiencing intense air pollution caused in large part by anthropogenic emissions of reactive nitrogen. These emissions result in the deposition of atmospheric nitrogen (N) in terrestrial and aquatic ecosystems, with implications for human and ecosystem health, greenhouse gas balances and biological diversity. However, information on the magnitude and environmental impact of N deposition in China is limited. Here we use nationwide data sets on bulk N deposition, plant foliar N and crop N uptake (from long-term unfertilized soils) to evaluate N deposition dynamics and their effect on ecosystems across China between 1980 and 2010. We find that the average annual bulk deposition of N increased by approximately 8 kilograms of nitrogen per hectare ($P < 0.001$) between the 1980s (13.2 kilograms of nitrogen per hectare) and the 2000s (21.1 kilograms of nitrogen per hectare). Nitrogen deposition rates in the industrialized and agriculturally intensified regions of China are as high as the peak levels of deposition in northwestern Europe in the 1980s, before the introduction of mitigation measures. Nitrogen from ammonium (NH4(+)) is the dominant form of N in bulk deposition, but the rate of increase is largest for deposition of N from nitrate (NO3(-)), in agreement with decreased ratios of NH3 to NOx emissions since 1980. We also find that the impact of N deposition on Chinese ecosystems includes significantly increased plant foliar N concentrations in natural and semi-natural (that is, non-agricultural) ecosystems and increased crop N uptake from long-term-unfertilized croplands. China and other economies are facing a continuing challenge to reduce emissions of reactive nitrogen, N deposition and their negative effects on human health and the environment.

The draft genome of the fast-growing non-timber forest species moso bamboo (Phyllostachys heterocycla). [地址链接**]**

通讯作者：韩斌&江泽慧(中国林业科学研究院) Nat Genet. 2013 Feb 24.

Bamboo represents the only major lineage of grasses that is native to forests and is one of the most important non-timber forest products in the world. However, no species in the Bambusoideae subfamily has been sequenced. Here, we report a high-quality draft genome sequence of moso bamboo (P. heterocycla var. pubescens). The 2.05-Gb assembly covers 95% of the genomic region. Gene prediction modeling identified 31,987 genes, most of which are supported by cDNA and deep RNA sequencing data. Analyses of clustered gene families and gene collinearity show that bamboo underwent whole-genome duplication 7-12 million years ago. Identification of gene families that are key in cell wall biosynthesis suggests that the whole-genome duplication event generated more gene duplicates involved in bamboo shoot development. RNA sequencing analysis of bamboo flowering tissues suggests a potential connection between drought-responsive and flowering genes.

PI(4,5)P2 5-phosphatase A regulates PI3K/Akt signalling and has a tumour suppressive role in human melanoma. [地址链接**]**

通讯作者：张旭东 (安徽医科大学) Nat Commun. 2013 Feb 26;4:1508.

Inositol polyphosphate 5-phosphatases can terminate downstream signalling of phosphatidylinositol-3 kinase; however, their biological role in the pathogenesis of cancer is controversial. Here we report that the inositol polyphosphate 5-phosphatase, phosphatidylinositol 4,5-bisphosphate 5-phosphatase, has a tumour suppressive role in melanoma. Although it is commonly downregulated in melanoma, overexpression of phosphatidylinositol 4,5-bisphosphate 5-phosphatase blocks Akt activation, inhibits proliferation and undermines survival of melanoma cells in vitro, and retards melanoma growth in a xenograft model. In contrast, knockdown of phosphatidylinositol 4,5-bisphosphate 5-phosphatase results in increased proliferation and anchorage-independent growth of melanocytes. Although DNA copy number loss is responsible for downregulation of phosphatidylinositol 4,5-bisphosphate 5-phosphatase in a proportion of melanomas, histone hypoacetylation mediated by histone deacetylases HDAC2 and HDAC3 through binding to the transcription factor Sp1 at the PIB5PA gene promoter appears to be another commonly involved mechanism. Collectively, these results establish the tumour suppressive role of phosphatidylinositol 4,5-bisphosphate 5-phosphatase and reveal mechanisms involved in its downregulation in melanoma.

S-nitrosylation of phosphotransfer proteins represses cytokinin signaling. [地址链接**]**

通讯作者：左建儒(中国科学院遗传与发育生物学研究所&中国科学院大学) at Commun. 2013 Feb 26;4:1529.

Cytokinin is an essential phytohormone in plant growth and development. In Arabidopsis, cytokinin signalling is mediated by a phosphorelay that sequentially transfers phosphoryl groups from the cytokinin receptors to histidine phosphotransfer proteins (AHPs) and response regulators (ARRs). However, little is known about the regulatory mechanism of the phosphorelay. Here, we show that nitric oxide negatively regulates cytokinin signalling by inhibiting the phosphorelay activity through S-nitrosylation. S-nitrosylation of AHP1 at Cys 115 represses its phosphorylation and subsequent transfer of the phosphoryl group to ARR1. A non-nitrosylatable mutation of AHP1 renders the mutant protein insensitive to nitric oxide in repressing its phosphorylation, and partially relieves the inhibitory effect of nitric oxide on the cytokinin response. Conversely, a nitrosomimetic mutation of AHP1 causes reduced phosphorylation of AHP1 and ARR1, thereby resulting in a compromised cytokinin response. These findings illustrate a mechanism by which redox signalling and cytokinin signalling coordinate plant growth and development.

Porous materials with pre-designed single-molecule traps for CO(2) selective adsorption. **[**地址链接**]**

通讯作者：Hong-Cai Zhou (北京科技大学) Nat Commun. 2013 Feb 26;4:1538

Despite tremendous efforts, precise control in the synthesis of porous materials with pre-designed pore properties for desired applications remains challenging. Newly emerged porous metal-organic materials, such as metal-organic polyhedra and metal-organic frameworks, are amenable to design and property tuning, enabling precise control of functionality by accurate

design of structures at the molecular level. Here we propose and validate, both experimentally and computationally, a precisely designed cavity, termed a 'single-molecule trap', with the desired size and properties suitable for trapping target CO(2) molecules. Such a single-molecule trap can strengthen CO(2)-host interactions without evoking chemical bonding, thus showing potential for CO(2) capture. Molecular single-molecule traps in the form of metal-organic polyhedra are designed, synthesised and tested for selective adsorption of CO(2) over N(2) and CH(4), demonstrating the trapping effect. Building these pre-designed single-molecule traps into extended frameworks yields metal-organic frameworks with efficient mass transfer, whereas the CO(2) selective adsorption nature of single-molecule traps is preserved.

A low-temperature method to produce highly reduced graphene oxide. **[**地址链接**]**

通讯作者：段镶锋&李景虹(清华大学) Nat Commun. 2013 Feb 26;4:1539

Chemical reduction of graphene oxide can be used to produce large quantities of reduced graphene oxide for potential application in electronics, optoelectronics, composite materials and energy-storage devices. Here we report a highly efficient one-pot reduction of graphene oxide using a sodium-ammonia solution as the reducing agent. The solvated electrons in sodium-ammonia solution can effectively facilitate the de-oxygenation of graphene oxide and the restoration of π-conjugation to produce reduced graphene oxide samples with an oxygen content of 5.6 wt%. Electrical characterization of single reduced graphene oxide flakes demonstrates a high hole mobility of 123 cm(2) Vs(-1). In addition, we show that the pre-formed graphene oxide thin film can be directly reduced to form reduced graphene oxide film with a combined low sheet resistance (~350 Ω per square with ~80% transmittance). Our study demonstrates a new, low-temperature solution processing approach to high-quality graphene materials with lowest sheet resistance and highest carrier mobility.

Excitation-dependent visible fluorescence in decameric nanoparticles with monoacylglycerol cluster chromophores. **[**地址链接**]**

通讯作者：李冠明(国立高雄师范大学) Nat Commun. 2013 Feb 26;4:1544.

Organic fluorescent nanoparticles, excitation-dependent photoluminescence, hydrogen-bonded clusters and lysobisphosphatidic acid are four interesting individual topics in materials and biological sciences. They have attracted much attention not only because of their unique properties and important applications, but also because the nature of their intriguing phenomena remained unclear. Here we report a new type of organic fluorescent nanoparticles with intense blue and excitation-dependent visible fluorescence in the range of 410-620 nm. The nanoparticles are composed of ten bis(monoacylglycerol)bisphenol-A molecules and the self-assembly occurs only in elevated concentrations of 2-monoacylglycerol via radical-catalysed 3,2-acyl migration from 3-monoacylglycerol in neat conditions. The excitation-dependent fluorescence behaviour is caused by chromophores composed of hydrogen-bonded monoacylglycerol clusters, which are linked by an extensive hydrogen-bonding network between the ester carbonyl groups and the protons of the alcohols with collective proton motion and HO ••• C=O (n→ π *) interactions.

Nuclear safety lies in greater transparency. **[**地址链接**]**

通讯作者：Wang Q. (中国科学院新疆生态与地理研究所) Nature. 2013 Feb 28;494(7438):403

No abstract.

Specialized appendages in fuxianhuiids and the head organization of early euarthropods. **[**地址链接**]**

通讯作者：张喜光(云南大学) Nature. 2013 Feb 28;494(7438):468-71.

The organization of the head provides critical data for resolving the phylogenetic relationships and evolutionary history of extinct and extant euarthropods. The early Cambrian-period fuxianhuiids are regarded as basal representatives of stem-group Euarthropoda, and their anterior morphology therefore offers key insights for reconstructing the ancestral condition of the euarthropod head. However, the paired post-antennal structures in Fuxianhuia protensa remain controversial; they have been interpreted as both 'great appendages' and as gut diverticulae. Here we describe Chengjiangocaris kunmingensis sp. nov. and Fuxianhuia xiaoshibaensis sp. nov. from a new early Cambrian (Stage 3) fossil Lagerstätte in Yunnan, China. Numerous specimens of both species show a unique 'taphonomic dissection' of the anterodorsal head shield, revealing the cephalic organization in detail. We demonstrate the presence of a pair of specialized post-antennal appendages (SPAs) in the fuxianhuiid head, which attach at either side of the posteriorly directed mouth, behind the hypostome. Preserved functional articulations indicate a well-defined but restricted range of limb movement, suggestive of a simple type of sweep feeding. The organization of the SPAs in fuxianhuiids is incompatible with the (deutocerebral) anterior raptorial appendages of megacheirans, and argue against the presence of protocerebral limbs in the fuxianhuiids. The positions of the fuxianhuiid antennae and SPAs indicate that they are segmentally homologous to the deutocerebral and tritocerebral appendages of crown-group Euarthropoda respectively. These findings indicate that antenniform deutocerebral appendages with many podomeres are a plesiomorphic feature of the ancestral euarthropod head.

2、Cell 及其子刊

Repression of the Long Noncoding RNA-LET by Histone Deacetylase 3 Contributes to Hypoxia-Mediated Metastasis. [地址链接**]**

通讯作者：汪方&孙树汉 (上海第二军医大学) Mol Cell. 2013 Feb 5. pii: S1097-2765(13)00043-9.

Recently, long noncoding RNAs (lncRNAs) were found to be dysregulated in a variety of tumors. However, it remains unknown how and through what molecular mechanisms the expression of lncRNAs is controlled. In this study, we found that the lncRNA Low Expression in Tumor

(lncRNA-LET) was generally downregulated in hepatocellular carcinomas, colorectal cancers, and squamous-cell lung carcinomas. We demonstrated that hypoxia-induced histone deacetylase 3 repressed lncRNA-LET by reducing the histone acetylation-mediated modulation of the lncRNA-LET promoter region. Interestingly, the downregulation of lncRNA-LET was found to be a key step in the stabilization of nuclear factor 90 protein, which leads to hypoxia-induced cancer cell invasion. Moreover, the relationship among hypoxia, histone acetylation disorder, low lncRNA-LET expression level, and metastasis was found in clinical hepatocellular carcinoma samples. These results advance our understanding of the role of lncRNA-LET as a regulator of hypoxia signaling and offer new avenues for therapeutic intervention against cancer progression.

Chromatic Coding from Cone-type Unselective Circuits in the Mouse Retina. [地址链接]

通讯作者：Thomas Euler (中国科学院生物物理研究所&中国科学院大学) Neuron, Volume 77, Issue 3, 559-571, 6

Retinal specializations such as cone-photoreceptor opsin-expression gradients, as found in several vertebrate species, are intuitively considered detrimental to color vision. In mice, the majority of cones coexpress both "blue" and "green" opsin. The coexpression ratio changes along the dorsoventral axis, resulting in a "green"-dominant dorsal and a "blue"-dominant ventral retina. Here, we asked how these specializations affect chromatic processing, especially with respect to the opsin transitional zone, the band where opsin coexpression shifts from "green" to "blue." Using electrophysiology, modeling, and calcium imaging, we found that "alpha-like" retinal ganglion cells, which previously have not been implicated in chromatic processing, display color-opponent responses when located in the vicinity of the opsin transitional zone. Moreover, direction-selective ganglion cells within this zone respond differentially to color sequences. Our data suggest that the dorsoventral opsin distribution, in combination with conventional spatiotemporal processing, renders mouse ganglion cell responses color-opponent without requiring cone-type selective connectivity.

MicroRNA-92a Upholds Bmp Signaling by Targeting noggin3 during Pharyngeal Cartilage Formation. [地址链接]

通讯作者：孟安明 &王强(中国科学院动物研究所) Dev Cell. 2013 Feb 11;24(3):283-95.

Craniofacial malformations are common structural birth defects and usually associate with abnormal development of pharyngeal arches. Although some microRNAs have been found to be implicated in chondrogenesis in vitro, few have been shown to be essential for cartilage and bone development at the whole organism level. In this study, we report that mir92a is highly enriched in the chondrogenic progenitors and that its inactivation results in loss of pharyngeal cartilage elements due to poor proliferation, impaired differentiation, and unsustainable survival of chondrogenic progenitors. The Bmp antagonist gene noggin3 (nog3) is a direct target of mir92a. Inactivation of mir92a stabilizes nog3 mRNA, leading to repression of Bmp signaling and abnormal behaviors of chondrogenic progenitors. In contrast, ectopic expression of mir92a duplex decreases nog3 mRNA levels and, as a result, derepresses Bmp signaling and promotes cell

apoptosis. Therefore, mir92a acts to maintain Bmp activity during pharyngeal cartilage formation by targeting nog3.

Hsp90 Regulates Nongenetic Variation in Response to Environmental Stress. [地址链接]

通讯作者：Jun-Yi Leu (中央研究院分子生物学研究所) Mol Cell. 2013 Feb 19. pii: S1097-2765(13)00090-7.

Nongenetic cell-to-cell variability often plays an important role for the survival of a clonal population in the face of fluctuating environments. However, the underlying mechanisms regulating such nongenetic heterogeneity remain elusive in most organisms. We report here that a clonal yeast population exhibits morphological heterogeneity when the level of Hsp90, a molecular chaperone, is reduced. The morphological heterogeneity is driven by the dosage of Cdc28 and Cla4, a key regulator of septin formation. Low Hsp90 levels reduce Cla4 protein stability and cause a subpopulation of cells to switch to a filamentous form that has been previously suggested to be beneficial under certain hostile environments. Moreover, Hsp90-dependent morphological heterogeneity can be induced by environmental stress and is conserved across diverse yeast species. Our results suggest that Hsp90 provides an evolutionarily conserved mechanism that links environmental stress to the induction of morphological diversity.

Structure of the MST4 in Complex with MO25 Provides Insights into Its Activation Mechanism. [地址链接]

通讯作者：赵允&周兆才(中国科学院上海生命科学研究院) Structure. 2013 Mar 5;21(3):449-61.

Mammalian STE20-like kinase MST4 regulates multiple cellular aspects such as cell polarity and proliferation. MST4 acts downstream of LKB1/MO25/STRAD complex to induce brush border formation. MO25 directly interacts with MST4 to promote its kinase activity. Here, we report the crystal structure of MST4 in complex with MO25. Association of MO25 rotates the αC helix of MST4 toward its catalytic core, stabilizing the αC helix in an active position. The kinase domain of MST4 forms a specific homodimer that is required for trans-autophosphorylation. MO25-stimulated activation of MST4 promotes apoptosis in HEK293T cells. Atomic resolution permitted the study of interface mutations capable of disrupting the MST4-MO25 interaction or the kinase-domain-mediated homodimerization. These mutations impaired MST4 kinase activation and function within the cell. Collectively, our study identifies the activation mechanism of MST4 and provides a structural basis for further functional study.

Structural insight into inactivation of plasminogen activator inhibitor-1 by a small-molecule antagonist. [地址链接]

通讯作者：黄明东 (中国科学院福建物质结构研究所) Chem Biol. 2013 Feb 21;20(2):253-61.

Plasminogen activator inhibitor-1 (PAI-1), a serpin, is the physiological inhibitor of tissue-type

and urokinase-type plasminogen activators and thus also an inhibitor of fibrinolysis and tissue remodeling. It is a potential therapeutic target in many pathological conditions, including thrombosis and cancer. Several types of PAI-1 antagonist have been developed, but the structural basis for their action has remained largely unknown. Here we report X-ray crystal structure analysis of PAI-1 in complex with a small-molecule antagonist, embelin. We propose a mechanism for embelin-induced rapid conversion of PAI-1 into a substrate for its target proteases and the subsequent slow conversion of PAI-1 into an irreversibly inactivated form. Our work provides structural clues to an understanding of PAI-1 inactivation by small-molecule antagonists and an important step toward the design of drugs targeting PAI-1.

3、Science 及其子刊

Sterical Hindrance Promotes Selectivity of the Autophagy Cargo Receptor NDP52 for the Danger Receptor Galectin-8 in Antibacterial Autophagy. [地址链接]

通讯作者：施蕴渝 (中国科技大学) Sci Signal. 2013 Feb 5;6(261):ra9.

Autophagy, the process of lysosome-dependent degradation of cytosolic components, is a mechanism by which cells selectively engulf invading pathogens to protect themselves against infection. Galectin-8, a cytosolic protein with specificity for β-galactoside-containing glycans, binds endosomal and lysosomal membranes that have been damaged, for example, by pathogens, and selectively recruits the autophagy cargo receptor NDP52 to induce autophagy. We solved the crystal structure of the NDP52-galectin-8 complex to show how NDP52 exclusively binds galectin-8 and, consequently, why other galectins do not restrict the growth of Salmonella in human cells.

Melamine-induced renal toxicity is mediated by the gut microbiota. [地址链接]

通讯作者：贾伟 (上海交通大学) Sci Transl Med. 2013 Feb 13;5(172):172ra22.

Melamine poisoning has become widely publicized after a recent occurrence of renal injury in infants and children exposed to melamine-tainted milk in China. This renal damage is believed to result from kidney stones formed from melamine and uric acid or from melamine and its cocrystallizing chemical derivative, cyanuric acid. However, the composition of the stones and the mechanism by which the stones are formed in the renal tubules are unknown. We report that cyanuric acid can be produced in the gut by microbial transformation of melamine and serves as an integral component of the kidney stones responsible for melamine-induced renal toxicity in rats. Melamine-induced toxicity in rats was attenuated, and melamine excretion decreased after antibiotic suppression of gut microbial activity. We further demonstrated that melamine is converted to cyanuric acid in vitro by bacteria cultured from normal rat feces; Klebsiella was subsequently identified in fecal samples by 16S ribosomal DNA sequencing. In culture, Klebsiella terrigena was shown to convert melamine to cyanuric acid directly. Rats colonized by K. terrigena showed exacerbated melamine-induced nephrotoxicity. Cyanuric acid was detected in the kidneys of rats administered melamine alone, and the concentration after Klebsiella colonization was

increased. These findings suggest that the observed toxicity of melamine may be conditional on the exact composition and metabolic activities of the gut microbiota.